Journal of Applied Veterinary Sciences, 10 (4): 96 -103 (October, 2025).
ISSN: Online: 2090-3308, Print: 1687-4072
Journal homepage : https://javs.journals.ekb.eg

Histological and Transcriptional Profiling Reveals Chondro-Osteogenic Trans-differentiation in Meniscal Mineralisation of the Domestic Cat (*Felis catus*)

Nur Izzati Inani ZABIDDIN[1], Md Zuki ABU BAKAR[1], Mohd Akmal MOHD NOOR[1], Mohd Faizal GHAZALI[2,3], Min Hian CHAI[2]and Siti Mariam ZAINAL ARIFFIN[1,*]

[1]Department of Veterinary Preclinical Sciences, Faculty of Veterinary Medicine, Universiti Putra Malaysia, Malaysia
[2]Faculty of Veterinary Medicine, Universiti Sultan Zainal Abidin, Malaysia
[3]Halal Research Centre, Universiti Sultan Zainal Abidin, Malaysia
***Corresponding Author:** Siti Mariam ZAINAL ARIFFIN, **E-Mail :** sitimariam_za@upm.edu.my

ABSTRACT

Meniscal mineralisation is commonly observed in domestic cats. However, its biological significance and underlying mechanisms remain unclear. This study aimed to characterise the histomorphological features of meniscal mineralisation and evaluate the mRNA expression of key chondro-osteogenic trans-differentiation markers in the feline meniscus. A total of 20 menisci (10 mineralised and 10 non-mineralised) were collected from skeletally mature domestic cats with disease-free joints following gross examination, during which meniscal mineralisation was identified. Both mineralised and non-mineralised menisci were collected for subsequent histological and molecular evaluation. Histological examination with H&E and Alizarin Red staining revealed that mineralisation was confined to the cranial horn of the medial meniscus, with most mineralised tissues displaying chondro-osseous metaplasia. The mean area of the mineralised regions was 276.9 ± 227.9 mm². Only one sample exhibited intrameniscal ossification, characterised by trabecular bone and bone marrow spaces. The lateral menisci showed no evidence of mineralisation. Cellular density was not significantly different between groups (p=0.232). Quantitative PCR analysis revealed significantly increased expression of mRNA for *COL10A1*, *MMP-13*, *TNAP*, *RunX*2, and *Sox*9 in mineralised menisci compared to controls (p<0.001), with *COL10A1* and *MMP-13* showing 9- to 7-fold increases, respectively. These genes were associated with hypertrophic chondrocyte differentiation, extracellular matrix remodelling and mineral deposition, indicating an active chondro-osteogenic trans-differentiation process. Collectively, the findings provide novel evidence that a chondro-osteogenic trans-differentiation pathway drives meniscal mineralisation in the domestic cat. This study enhances the understanding of meniscal biology in felines and may offer insights into joint mineralisation processes across species.

Original Article:
DOI:10.21608/javs.2025.416539.1717
Received : 22 August, 2025.
Accepted: 29 September, 2025.
Published in October, 2025.

Keywords: Chondro-osteogenictrans-differentiation, Feline, Histology, Meniscal mineralisation, Stifle joint.

J. Appl. Vet. Sci., 10(4): 96-103.

INTRODUCTION

Meniscal mineralisation refers to the deposition of calcium crystals within the meniscus. It is commonly observed in domestic cats and has also been reported in large non-domestic felids (**Ganey *et al*., 1994; Walker *et al*., 2002; Arencibia *et al*., 2015**). Although meniscal mineralisation is often considered a normal anatomical feature, present as a sesamoid structure known as the lunula that forms during skeletal maturation, its exact cause remains unclear (**Whiting and Pool, 1985; Ariffin, 2015**). Notably, previous studies have reported a correlation between meniscal mineralisation and cartilage degeneration within the feline stifle (**Leijon *et al*., 2017**).

Meniscal mineralisation morphology is variable, with some studies describing it as trabecular bone formation containing marrow spaces, while others report regions of chondro-osseous metaplasia (**Freire *et***

***al*., 2010; Ariffin, 2015; Voss *et al*., 2017**). A major challenge in characterising meniscal mineralisation is its inter-individual size variability, which has not been consistently documented. This limits the understanding of its morphological features and potential impact on joint health. The meniscus typically presents as a smooth, fibrocartilaginous structure without mineral deposits. These joints are generally stable and demonstrate a full range of motion. In contrast, stifle joints affected by degenerative meniscal changes often exhibit lesions such as mineralisation, surface fibrillation and tearing of the meniscal tissue (**Ariffin, 2015; Voss *et al*., 2017**). Such alterations are frequently accompanied by osteoarthritic changes in the stifle joint that affect joint mobility and pain.

Emerging evidence suggests that mineralisation in various tissues may involve active cellular processes such as trans-differentiation. Mesenchymal stem cells, for instance, can acquire an osteogenic phenotype in response to environmental cues (**Javaheri *et al*., 2018**). Similar mechanisms have been reported in vascular calcification and tendinopathy, where smooth muscle cells and tenocytes transdifferentiate into hypertrophic chondrocytes or osteoblast-like cells (**Bobryshev, 2005; Pillai *et al*., 2017; Darrieutort-Laffite *et al*., 2019**). These processes are typically associated with the upregulation of transcription factors such as Runt-related transcription factor 2 (*RunX*2), SRY-box transcription factor 9 (*Sox*9), Tissue-nonspecific alkaline phosphatase (*TNAP*), matrix metallopeptidase 13 (*MMP-13*), and collagen type X alpha 1 chain (*COL10A1*). To date, the molecular mechanisms underlying meniscal fibrochondrocyte-to-osteoblast differentiation in felines remain unexplored.

This study aimed to characterise the histomorphological features of meniscal mineralisation. Additionally, the study investigates the expression levels of key chondro-osteogenic indicators in mineralised and non-mineralised menisci of domestic cats.

MATERIALS AND METHODS

Cat cadaver

Twenty skeletally mature domestic cat carcasses submitted to the Faculty of Veterinary Medicine, Universiti Putra Malaysia, were included in the study. All animals were euthanised due to causes not associated with this research. The inclusion criteria required that cats were at least one year of age, as skeletal maturity is generally reached by 12-18 months in domestic cats **(Miranda *et al.,* 2020)** and had a body condition score of 3. Additionally, the stifle joints had to be intact, free from tibiofemoral osteoarthritis, meniscal degeneration and cranial cruciate ligament rupture.

Dissection of the stifle joint

Cat carcasses were dissected within 24 hours post-mortem. The stifle joint was palpated to identify anatomical landmarks. The overlying fascia and fat were reflected, and the patellar and collateral ligaments were resected. A lateral incision was made in the joint capsule to access the joint cavity, followed by careful resection of the cruciate ligaments near their femoral attachments to preserve integrity. The meniscus was examined *in situ* to assess for mineralisation. If present and grossly visible, the mineralised region was measured in millimetres using a digital calliper.

Sample collection

Twenty representative menisci (10 mineralised and 10 non-mineralised) were obtained and immersed in 10% neutral buffered formalin for histomorphological analysis. For gene expression analysis, 38 representative meniscal samples (19 mineralised and 19 non-mineralised) were immersed in RNAlater™ solution (Sigma-Aldrich®, US), incubated at 4 ºC for 24 hours and subsequently stored at –20 ºC to preserve ribonucleic acid (RNA) stability until further processing. The non-mineralised menisci served as the control group.

Histological preparation and staining

Meniscal tissues were processed for histological evaluation using standard protocols. Horizontal sections measuring 5.0 µm in thickness were performed. Routine histological staining was conducted using haematoxylin and eosin (H&E) staining (Solarbio® Life Sciences, China) for morphological assessment. Meniscal samples exhibiting evidence of mineralisation were subjected to staining with 1% Alizarin Red solution (Solarbio® Life Sciences, China). Tissue sections were first deparaffinised and rehydrated through immersion in xylene, followed by a graded alcohol series (100% to 70%). The sections were then air-dried and incubated with 1% Alizarin Red solution (pH 4.2) for one minute. After staining with distilled water to remove excess dye, the sections were dehydrated, cleared and mounted in DPX medium (Sigma-Aldrich®, USA).

Histomorphological and histomorphometrical analysis

Tissue sections were examined and imaged using a Motic BA410 light microscope fitted with a Moticam Pro 285A camera (Xiamen, China). The histomorphological features of meniscal mineralisation were qualitatively evaluated in both H&E- and Alizarin red-stained sections. ImageJ software (developed by the National Institutes of Health, USA) was used for analysis, focusing on two parameters: the dimensions of mineralised regions and cellular density. H&E-stained

sections were imaged at a total magnification of 100× for both studies. The areas of mineralisation (mm^2) were measured using the digital ruler tool in ImageJ. For cellular density, five representative images were captured from each of the meniscal regions (cranial, middle, and caudal thirds). Cell nuclei were identified and manually marked using the multipoint tool in ImageJ. Cell density was defined as the number of cells present within a 1.50 mm^2 tissue section (**Fedje-Johnston *et al*., 2021**).

Chondro-osteogenic transdifferentiation gene expression

Meniscal samples preserved in RNAlater™ were frozen in liquid nitrogen and finely ground using a mortar and pestle, and 30 mg of tissue was subjected to total RNA isolation with the InnuPREP RNA Mini Kit (Analytik Jena, Germany). Lysates were homogenised using a 21-gauge needle, followed by centrifugation at 14,000 rpm for 1 minute at 20 °C. Total RNA was eluted in 50 µl of RNase-free water. RNA concentration and purity were determined using a NanoDROP ND-1000 Spectrophotometer (Thermo Scientific, UK), accepting only samples with A260/A280 values ranging from 1.8 to 2.0 for complementary DNA (cDNA) synthesis. The SensiFAST™ cDNA Synthesis Kit (Meridian Bioscience, USA) was used to synthesise cDNA from 6 ng of total RNA, with reverse transcription performed at 48 °C for 30 minutes. Primers for *Run*X2, *Sox*9, *TNAP*, *MMP-13*, and *COL10A1* were designed based on feline mRNA sequences using the Primer-BLAST tool (NCBI) and were commercially produced. Primers were selected based on similar melting temperatures and product lengths. The primer sequences are shown in **Table 1**.

Table 1: qPCR primer sequences for chondro-osteogenic markers and reference genes.

Target genes	Nucleotide sequence (5′→ 3′)	Amplicon size (bp)
***RunX*2**	F: TCCGAAATGCCTCTG CTG TTA	120
	R: GGGAGGGTTTGTGAAGACAGT	
***Sox*9**	F: GGAGACTGCTGAACGAGAGC	128
	R: GCCGTTCTTCACCGACTTCC	
TNAP	F: CCGCCTACTTATGTGGGGTC	145
	R: ATGCCCACAGATTTGCCAGA	
***MMP*-13**	F: AAT CCT GAA GAA AGC GGC CA	157
	R: AAC GTT GTA CTC GCC CAC AT	
COL10A1	F: CAT CAA AGG TGA TCG GGG CT	158
	R: CAG GGT GAC CTT TTG TCC CA	
HPRT	F: AACTGGAAAGAATGTCTTGATTGTTG	132
	: GACCATCTTTGGATTATACTGCTTGA	

The qPCR was carried out with the SensiFAST™ SYBR® No-Rox One-Step Kit (Meridian Bioscience, USA). The qPCR reaction mixture (20 µl) contained 10 µl of master mix, 0.8 µl of each primer (forward and reverse), 7.4 µl RNase-free water, and 1 µl of cDNA at a concentration of 1 ng/µl. Reactions were run in triplicate in 8-well PCR strip tubes (Labcon®, USA). Non-template and minus-RT controls were included. Using the Eppendorf® Realplex 4 system, amplification was performed with an initial step at 95 °C for 2 minutes, followed by 40 cycles consisting of 95 °C for 5 seconds, 62 °C for 10 seconds, and 72 °C for 20 seconds. Specificity of amplification was verified through melting curve analysis, and samples displaying abnormal or multiple peaks were excluded. Target gene expression was analysed using triplicate cycle threshold (Ct) values, normalised to the reference gene hypoxanthine phosphoribosyl transferase (HPRT). Relative fold changes were calculated using the ΔΔCt method.

Statistical analysis

Data for cell density and mRNA expression levels between mineralised and non-mineralised menisci were assessed for normality using the Shapiro-Wilk test. An independent t-test was applied to compare mean cell densities and mRNA expression levels between mineralised and non-mineralised menisci. Differences were considered significant at $p<0.05$. All values are shown as mean ± SD.

RESULTS

Gross features of meniscal mineralisation

The mean age cats included was 3.0 ± 0.5 years. Gross examination revealed mineralisation localised to the cranial horn of the medial meniscus and appeared round to oval in shape, as shown in **Fig.1**. The mean diameter ranges from 0.1 to 1.50 mm. No mineralisation was observed in the lateral meniscus of any of the examined specimens.

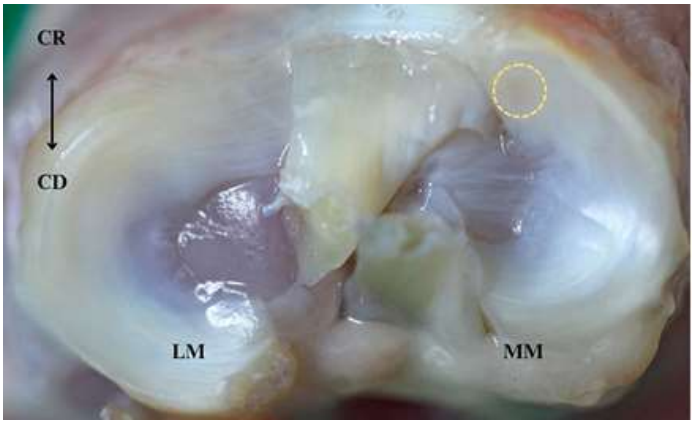

Fig.1: Photograph showing mineralisation within the meniscus of the left stifle joint in cats appears as round to oval-shaped opaque regions embedded in the cranial horn of the medial meniscus (MM) (yellow dotted circle). In contrast, non-mineralised lateral menisci (LM) appeared smooth and glossy, with no visible signs of mineral deposition. CR: cranial; CD: caudal.

Histomorphology of meniscal mineralisation

All 20 meniscal samples (10 mineralised and 10 non-mineralised) were stained with Alizarin Red to screen for the presence of calcium compounds. In mineralised samples, horizontal sections revealed round structures with distinct orange to red staining, indicating calcium deposition **(Fig. 2.A-B)**. In contrast, non-mineralised samples showed no evidence of Alizarin Red staining **(Fig. 2.C)**.

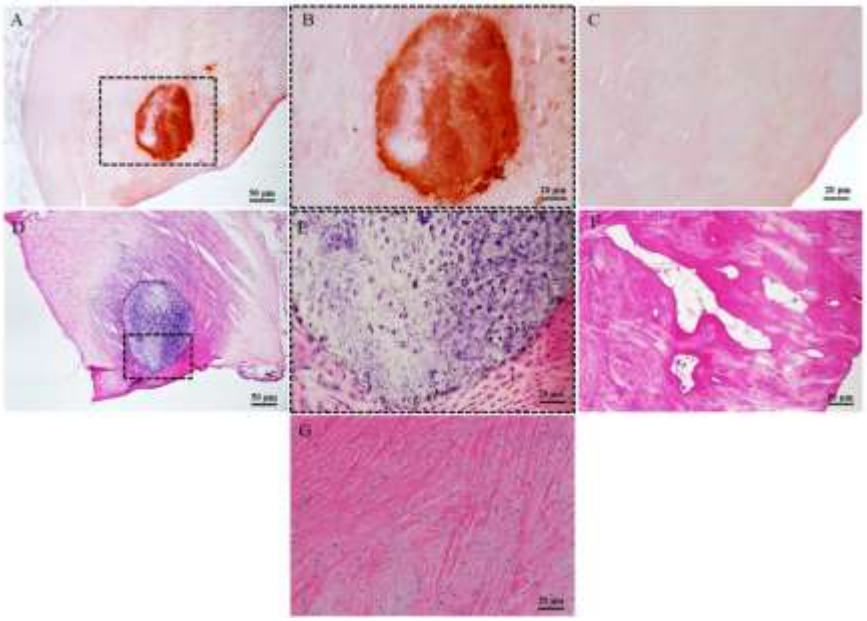

Fig. 2: Histological images showing horizontal sections of the cranial horn of the medial meniscus with meniscal mineralisation (A, B, D, E & F) in the left stifle joint of cats. The boxed areas in the lower magnification images are shown at higher magnification in B and E. (A-B) The mineralised meniscal tissue in the calcified area is stained orange to red, confirming the presence of calcium compounds. (C) Non-mineralised samples showed no evidence of Alizarin Red staining. (D) The meniscus displays mineralisation along with areas of chondro-osseous metaplasia. (E) Hypertrophic chondrocytes appear round to oval and reside within larger, irregular lacunae. Both the hypertrophic chondrocytes and the extracellular matrix exhibit strong basophilic staining. (F) Meniscal mineralisation showing trabecular bone and marrow spaces. (G) Interwoven fibrocartilage without mineralisation. The cells are arranged in rows or lines between the bundles of parallel collagen fibres. A-C: Alizarin Red; D-G: H&E. A, D & F: 40x magnification; B, C, E & G: 100x magnification.

Histological sections stained with H&E showed that 9 out of 10 mineralised meniscal samples exhibited areas of chondro-osseous metaplasia that appeared basophilic and were characterised by hypertrophic chondrocytes **(Fig. 2.D-E)**. The cells appeared round to oval, were spaced apart and resided in large, irregular lacunae. Only one of the ten mineralised meniscal samples showed intrameniscal ossification with the formation of trabecular bone and marrow spaces **(Fig. 2.F)**. All ten non-mineralised menisci showed no evidence of mineralisation **(Fig.2.G)**. The area of mineralised regions was assessed histomorphometrically, with a mean ± SD of 276.9 ± 227.9 mm².

Cellular density was calculated for both mineralised and non-mineralised menisci. Non-mineralised menisci showed a mean density of 0.28±0.10 cells/mm^2, while mineralised menisci had a mean of 0.23±0.04 cells/mm^2. Statistical analysis revealed no significant difference (p=0.232).

Chondro-osteogenic transdifferentiation gene expression

The expression of *COL10A1* in the mineralised samples was 9 times higher compared to non-mineralised menisci **(Fig.3.A)**. *COL10A1* mRNA expression was significantly elevated in the non-mineralised menisci (p<0.001), as shown in **Fig. 3.B**.

In the mineralised samples, the expression of *MMP-13* mRNA was 7-fold increased relative to the non-mineralised menisci **(Fig.3.C)**. Similar to *COL10A1*, *MMP-13* mRNA expression was significantly upregulated (p<0.001) in the mineralised samples compared to the non-mineralised menisci **(Fig. 3.D)**.

Additionally, *TNAP*, *RunX*2, and *Sox*9 mRNA levels were all upregulated in the mineralised samples. Each of these genes showed a 5-fold increase in expression in the mineralised samples compared to the non-mineralised menisci **(Fig.3.E, 3.G, 3.I)**. Mineralised samples exhibited significantly elevated mRNA levels of *TNAP*, *RunX*2, and *Sox*9 relative to non-mineralised menisci (p<0.001) **(Fig. 3.F, 3.H, 3.J)**.

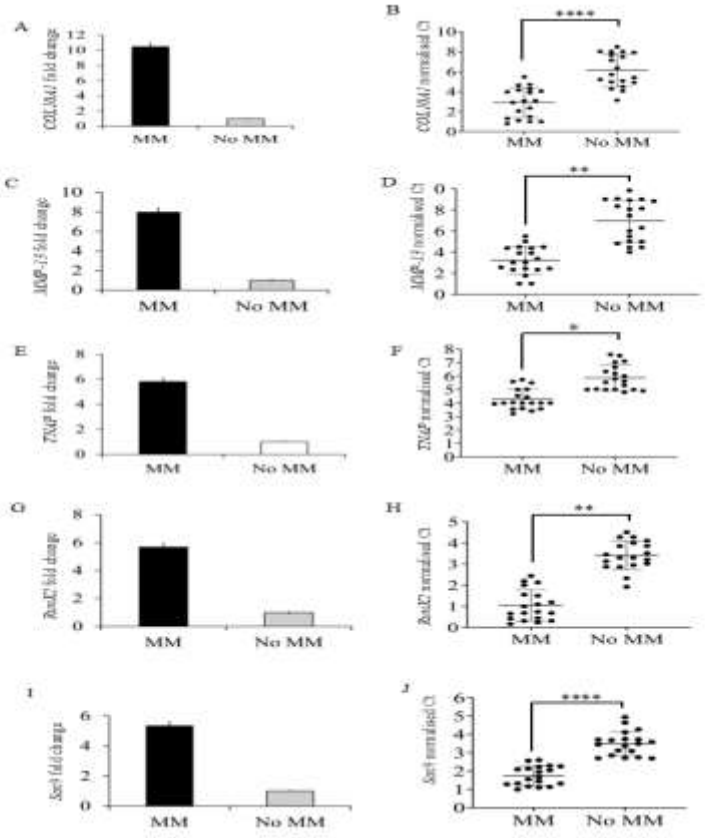

Fig. 3: Bar chart showing fold change and normalised Ct for five marker genes in mineralised (MM) and non-mineralised (No MM) menisci of cats. Fold change in *COL10A1* was 9 times higher with lower significance in normalised Ct (3.A and 3.B). *MMP-13* shows a 7-fold change with a lower significance difference in normalised Ct (3.C and 3.D). The fold changes in *TNAP*, *RunX*2, and *Sox*9 are the same, as shown in 3.E, 3.G, and 3.I, respectively, at a 5-fold increase. Normalised city for *TNAP*, *RunX*2, and *Sox*9 are significantly lower than the no MM sample shown in 3.F, 3.H, and 3.J, respectively.

DISCUSSION

The present study characterised meniscal mineralisation in healthy stifle joints of domestic cats, focusing on the associated cellular and molecular mechanisms. Histologically, in the present study, the mineralisation was evident as discrete calcifications and areas of chondro-osseous metaplasia. The areas of chondro-osseous metaplasia observed in this study are known to be associated with the mechanical stress of repetitive injury that occurs in the meniscus. Interestingly, these changes were only found in the medial meniscus, specifically the cranial horn, consistent with a previous study (**Freire *et al*., 2010**). The exact reason for this remains unclear. However, it is possible that increased mechanical loading is exerted on the medial compartment of the stifle joint, making it more susceptible to this transformation.

Prominent hypertrophy of fibrochondrocytes was also observed. Importantly, Alizarin Red staining distinctly marked these mineralised areas, confirming the presence and precise localisation of calcium-rich mineral deposits. As fibrochondrocytes undergo hypertrophy, they actively modify the extracellular matrix (ECM) by upregulating the production of type X collagen (*COL10A1*) and proteoglycans (**Debiais-Thibaud *et al*., 2019**). This newly synthesised proteoglycan-rich ECM, evidenced by basophilic staining (Figures 2.C-D), creates an environment conducive to vascular infiltration and facilitates the transition from fibrocartilage to bone (**Mwale *et al*., 2002; Dennis *et al*., 2020; Chen *et al*., 2023**).

Previous studies have shown that meniscal mineralisation can progress over time (**Voss *et al*., 2017**). They may increase in size and undergo ossification, resulting in the development of organised bone structures that include trabeculae and marrow spaces. This progression reflects a continuum from initial mineral deposition to the formation of mature bone tissue within the meniscus, a process more commonly observed in older animals or those with degenerative joint changes (**Voss *et al*., 2017**). In the present study, most samples were collected from cats with an average age of three years. Given their relatively young age, it is likely that these cats had not yet reached the advanced stages of mineralisation seen in older or degenerative cases. Consistent with this, only one sample exhibited mineralisation that had progressed to the point of forming trabecular bone and marrow spaces.

There was no significant variation in cellular density between mineralised and non-mineralised menisci in our study, suggesting that meniscal tissue is capable of maintaining a relatively stable cellular density, regardless of mineralisation status. The findings align with evidence that the meniscus contains specialised cell populations and homeostatic mechanisms that regulate cellularity and ECM composition. This is important to preserve tissue function under varying conditions (**Ding *et al*., 2022**).

The literature previously described feline meniscal mineralisation as presenting in the form of sesamoid bone, which is commonly accepted as a normal anatomical feature of the meniscus (**Whiting and Pool, 1985**). For example, in Pumas (*Felis concolor*), a sesamoid bone has been identified in the cranial horn of the medial meniscus, appearing histologically as spongy bone with sporadic osteons and an articular cartilage cap (**Cerveny and Paral, 1995)**. However, in the present study, none of the mineralised menisci exhibited features consistent with a sesamoid bone. Furthermore, no degenerative changes were observed in any of the samples, suggesting that the mineralisation identified in this study represents a non-pathological process in healthy feline stifle joints.

Chondro-osteogenic trans-differentiation is the process by which cartilage cells transition toward an osteogenic phenotype (**Aghajanian and Mohan, 2018**). Specific marker genes regulate this transformation, and each gene functions at a distinct stage of the process. The qPCR results demonstrated that *RunX*2, *Sox*9, *MMP-13*, *TNAP,* and *COL10A1* mRNA levels were significantly higher in mineralised menisci than in non-mineralised samples. This discovery is particularly relevant and new, considering the hypothesis that chondro-osseous trans-differentiation is involved in feline meniscal mineralisation.

COL10A1 (type X collagen) is primarily produced by hypertrophic chondrocytes and serves as a specific marker for the transition from cartilage to bone (**Gu *et al*., 2014**; **Debiais-Thibaud *et al*., 2019**). In this study, *COL10A1* expression increased nine-fold in mineralised samples, highlighting its role in initiating calcium deposition within the cartilaginous ECM (**Kirsch and Wuthier, 1994**). *MMP-13*, which showed a seven-fold increase, is responsible for degrading type II collagen in the matrix and plays a necessary step for ECM reorganisation and subsequent bone (**Duncan *et al*., 2022**).

Additionally, *RunX*2, *TNAP,* and *Sox*9 each exhibited a five-fold increase in expression. *RunX*2 is a key regulator of osteogenic differentiation and interacts with *Sox*9 to balance chondrogenesis and osteogenesis. *Sox*9 maintains chondrocyte function and prevents premature transition to osteoblast (**Lefebvre and Dvir-Ginzberg, 2017**). *TNAP* is crucial for mineralisation as it hydrolyses phosphate esters to release inorganic phosphate, which is needed for bone mineral formation (**Sekaran *et al*., 2021**).

CONCLUSIONS

This study confirms the presence of mineralisation in the healthy meniscus of domestic cats, particularly at the cranial horn of the medial meniscus. Histomorphological analysis revealed that the majority of the observed regions were chondro-osseous, as evidenced by positive staining with Alizarin Red, indicating mineralisation, along with one sample exhibiting trabecular bone with marrow. qPCR analysis revealed a marked upregulation of chondro-osteogenic trans-differentiation marker genes in mineralised menisci compared to non-mineralised menisci, strongly reinforcing the hypothesis that mineralisation in the feline meniscus is driven by chondro-osseous trans-differentiation.

Acknowledgment

This study was funded by Geran Inisiatif Putra Muda (GP-IPM) under the project code (GP-IPM/2022/9714600).

Conflict of interest

The authors declare that there are no conflicts of interest related to this study.

REFERENCES

AGHAJANIAN, P., and MOHAN, S., 2018. The art of building bone: emerging role of chondrocyte-to-osteoblast trans-differentiation in endochondral ossification. Bone Research, 6(1), 19. https://doi.org/10.1038/s41413-018-0021-z

ARENCIBIA, A., ENCINOSO, M., JÁBER, J. R., MORALES, D., BLANCO, D., ARTILES, A., and VÁZQUEZ, J. M., 2015. Magnetic resonance imaging study in a normal Bengal tiger (*Panthera tigris*) stifle joint. BMC Veterinary Research, 11(1), 192. https://doi.org/10.1186/s12917-015-0532-4

ARIFFIN, S. M. Z. 2015. Radiographic and pathologic studies of feline appendicular osteoarthritis. Ph.D. Dissertation, University of Glasgow, Scotland.

BOBRYSHEV, Y. V. 2005. Trans-differentiation of smooth muscle cells into chondrocytes in atherosclerotic arteries in situ: implications for diffuse intimal calcification. The Journal of Pathology, 205(5), 641–650. https://doi.org/10.1002/path.1743

CERVENY, C., and PARAL, V., 1995. Sesamoid bones of the knee joint of the *Puma concolor*. Acta Veterinaria Brno, 64(1), 79–82. https://doi.org/10.2754/avb199564010079

CHEN, N., WU, R. W. H., LAM, Y., CHAN, W. C. W., and CHAN, D., 2023. Hypertrophic chondrocytes at the junction of musculoskeletal structures. Bone Report, 19, 101698. https://doi.org/10.1016/j.bonr.2023.101698

DARRIEUTORT-LAFFITE, C., ARNOLFO, P., GARRAUD, T., ADRAIT, A., COUTÉ, Y., LOUARN, G., TRICHET, V., LAYROLLE, P., GOFF, B. L., and BLANCHARD, F., 2019. Rotator cuff tenocytes differentiate into hypertrophic chondrocyte-like cells to produce calcium deposits in an alkaline phosphatase-dependent manner. Journal of Clinical Medicine, 8(10), 1544. https://doi.org/10.3390/jcm8101544

DEBIAIS-THIBAUD, M., SIMION, P., VENTÉO, S., MUÑOZ, D., MARCELLINI, S., MAZAN, S., and HAITINA, T., 2019. Skeletal mineralization in association with type X collagen expression is an ancestral feature for jawed vertebrates. Molecular Biology and Evolution, 36(10), 2265-2276. https://doi.org/10.1093/molbev/msz145

DENNIS, J. E., WHITNEY, G. A., RAI, J., FERNANDES, R. J., and KEAN, T. J., 2020. Physioxia stimulates extracellular matrix deposition and increases the mechanical properties of human chondrocyte-derived tissue-engineered cartilage. Frontiers in Bioengineering and Biotechnology, 8, 590743. https://doi.org/10.3389/fbioe.2020.590743

DING, G., DU, J., HU, X., and AO, Y., 2022. Mesenchymal stem cells from different sources in meniscus repair and regeneration. Frontiers in Bioengineering and Biotechnology, 10, 796367. https://doi.org/10.3389/fbioe.2022.796367

DUNCAN, H. F., KOBAYASHI, Y., YAMAUCHI, Y., QUISPE-SALCEDO, A., FENG, Z. C., HUANG, J., PARTRIDGE, N. C., NAKATANI, T., D'ARMIENTO, J., and SHIMIZU, E., 2022. The critical role of *MMP-13* in regulating tooth development and reactionary dentinogenesis repair through the WNT signalling pathway. Frontiers in Cell and Developmental Biology, 10, 883266. https://doi.org/10.3389/fcell.2022.883266

FEDJE-JOHNSTON, W., TÓTH, F., ALBERSHEIM, M., CARLSON, C. S., SHEA, K. G., RENDAHL, A., and TOMPKINS, M., 2021. Changes in matrix components in the developing human meniscus. The American Journal of Sports Medicine, 49(1), 207-214. https://doi.org/10.1177/0363546520972418

FREIRE, M., BROWN, J., ROBERTSON, I. D., PEASE, A. P., HASH, J., HUNTER, S., SIMPSON, W., SUMRELL, A. T., and LASCELLES, B. D. X., 2010. Meniscal mineralisation in domestic cats. Veterinary Surgery, 39(5), 545–552. https://doi.org/10.1111/j.1532-950X.2010.00648.x

GANEY, T. M., OGDEN, J. A., ABOU-MADI, N., COLVILLE, B., ZDYZIARSKI, J. M., and OLSEN, J. H., 1994. Meniscal ossification: II. The normal pattern in the tiger knee. Skeletal Radiology, 23(3), 173-179. https://doi.org/10.1007/BF00197455

GU, J., LU, Y., LI, F., QIAO, L., WANG, Q., LI, N., BORGIA, J. A., DENG, Y., LEI, G., and ZHENG, Q., 2014. Identification and characterization of the novel *Col10a1* regulatory mechanism during chondrocyte hypertrophic differentiation. Cell Death & Disease, 5(10), e1469-e1469. https://doi.org/10.1038/cddis.2014.444

JAVAHERI, B., CAETANO-SILVA, S. P., KANAKIS, I., BOU-GHARIOS, G., and PITSILLIDES, A. A., 2018. The Chondro-osseous continuum: Is it possible to unlock the potential assigned within? Frontiers in Bioengineering and Biotechnology, 6, 28. https://doi.org/10.3389/fbioe.2018.00028

KIRSCH, T., and WUTHIER, R. E., 1994. Stimulation of calcification of growth plate cartilage matrix vesicles by

binding to type II and X collagens. The Journal of Biological Chemistry, 269(15), 11462–11469. https://doi.org/10.1016/S0021-9258(19)78146-0

LEFEBVRE, V., and DVIR-GINZBERG, M., 2017. *Sox9* and the many facets of its regulation in the chondrocyte lineage. Connective Tissue Research, 58(1), 2-14. https://doi.org/10.1080/03008207.2016.1183667

LEIJON, A., LEY, C. J., CORIN, A., and LEY, C., 2017. Cartilage lesions in feline stifle joints – associations with articular mineralisation and implications for osteoarthritis. Research in Veterinary Science, 114, 186–193. https://doi.org/ 10.1016/j.rvsc.2017.04.008

MIRANDA, F. G., SOUZA, I. P., VIEGAS, F. M., MEGDA, T. T., NEPOMUCENO, A. C., TÔRRES, R. C., and REZENDE, C. M. 2020. Radiographic study of the development of the pelvis and hip and the femorotibial joints in domestic cats. Journal of Feline Medicine and Surgery, 22(6), 476–483. https://doi: 10.1177/1098612X19854809

MWALE, F., TCHETINA, E., WU, C. W., and POOLE, A. R., 2002. The assembly and remodelling of the extracellular matrix in the growth plate in relationship to mineral deposition and cellular hypertrophy: an in-situ study of collagens II and IX and proteoglycan. Journal of Bone and Mineral Research, 17(2), 275–283. https://doi.org/10.1359/jbmr.2002.17.2.275

PILLAI, I. C. L., LI, S., ROMAY, M., LAM, L., LU, Y., HUANG, J., DILLARD, N., ZEMANOVA, M., RUBBI, L., WANG, Y., LEE, J., XIA, M., LIANG, O., XIE, Y. H., PELLEGRINI, M., LUIS, A. J.,and DEB, A., 2017. Cardiac fibroblasts adopt osteogenic fates and can be targeted to attenuate pathological heart calcification. Cell Stem Cell, 20(2), 218–232. https://doi.org/10.1016/j.stem.2016.10.005

SEKARAN, S., VIMALRAJ, S., and THANGAVELU L., 2021. The physiological and pathological role of tissue nonspecific alkaline phosphatase beyond mineralisation. Biomolecules, 11(11), 1564. https://doi.org/10.3390/biom1111

VOSS, K., KARLI, P., MONTAVON, P. M., GEYER, H., 2017. Association of mineralisation in the stifle joint of domestic cats with degenerative joint disease and cranial cruciate ligament pathology. Journal of Feline Medicine and Surgery, 19(1), 27–35. https://doi.org/10.1177/1098612X15606774

WALKER, M., PHALAN, D., JENSEN, J., JOHNSON, J., DREW, M., SAMII, V., HENRY, G. and MCCAULEY, J. 2002. Meniscal ossicles in large non-domestic cats. Veterinary Radiology & Ultrasound, 43(3), 249-254. https://doi.org/10.1111/j.1740-8261.2002.tb00998.x

WHITING, P. G., and POOL, R. R., 1985. Intrameniscal calcification and ossification in the stifle joints of three domestic cats. Journal of the American Animal Hospital Association, 21(4), 579–584.

How to cite this article:

Nur Izzati Inani ZABIDDIN, Md Zuki ABU BAKAR, Mohd Akmal MOHD NOOR, Mohd Faizal GHAZALI, Min Hian CHAI[2]and Siti Mariam ZAINAL ARIFFIN, 2025. Histological and Transcriptional Profiling Reveals Chondro-Osteogenic Trans-differentiation in Meniscal Mineralisation of the Domestic Cat (*Felis catus*). Journal of Applied Veterinary Sciences, 10 (4): 96-103. **DOI:10.21608/javs.2025.416539.1717**